ACS OMEGA

Article

Cite This: ACS Omega 2019, 4, 10799−10808

http://pubs.acs.org/journal/acsodf

Unraveling the Mechanistic Origins of Epoxy Degradation in Acids

Jacob Song Kiat Lim,*[,†,‡] Chee Lip Gan,[†,‡] and Xiao Matthew Hu*[,†,‡,§]

[†]School of Material Science and Engineering, Nanyang Technological University, Nanyang Avenue, 639798 Singapore, Singapore

[‡]Temasek Laboratories, Nanyang Technological University, 50 Nanyang Drive, 637553 Singapore

[§]Nanyang Environment and Water Research Institute, Nanyang Technological University, 637141 Singapore, Singapore

Supporting Information

ABSTRACT: Water diffusion into polymers like thermosetting epoxies is well-studied; however, comparably little has been reported thus far on the related but very different mechanism of acid diffusion and the corresponding influence on material degradation. The diffusion of hydrochloric acid into an amine-cured epoxy system was studied in this work using gravimetric analysis and dielectric monitoring concurrently, and the mass uptake behavior was observed to differ significantly compared with water diffusion, faster by an order of magnitude. A unique 3-stage diffusion of acid into epoxy was observed due to the influence of Coulombic interactions between oppositely charged ionic species diffusing at different rates. Material characterization studies have revealed that the dominant degradation mechanism is physical in nature, with the formation of surface cracks driven by the swelling stresses due to the core−shell swelling behavior in highly concentrated hydrochloric acid, leading to an erosion-type degradation phenomenon. The insights gained from understanding acid electrolyte diffusion could serve to design a more effective and efficient process to enable thermoset recycling by facilitating rapid material breakdown or the design of acid-resistant materials for various applications in chemical storage tanks, batteries, and protective coatings in a corrosive environment.

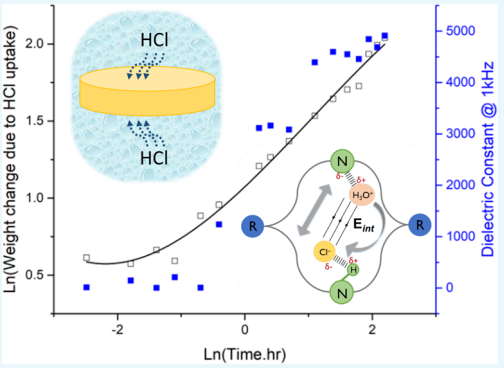

INTRODUCTION

Resource depletion and societies' difficulty in addressing the end-of-life management of cross-linked polymer products have led to trending research interests in related topics such as recyclable thermosets[1−4] and fiber recovery from composite wastes.[5] While most reported works focused on elucidating the enabling chemical reactions that permit controllable degradation, typically with acids and/or heat, the physical chemistry aspects of the diffusion-limited degradation process are poorly understood. Furthermore, since such materials are often used in their glassy state, the diffusion behavior of acids into glassy thermosets is expected to be similar, regardless of whether the polymer is designed to be degradable or not. Thermosetting epoxies are often the material of choice for applications handling corrosive media, but even then, the diffusion mechanism and the corresponding material degradation behavior are not well understood. Epoxy resins are considered among the top-line materials in terms of chemical corrosion resistance; however, most relevant investigations into the origin of chemical resistance tend to be restricted to qualitative evaluations such as those data published in material handbooks or chemical compatibility guides, which only provide a superficial insight into the environmental conditions and resistance duration.[6,7] In contrast to the common assumption that acid degradation is a chemical degradation process, it was realized through this work that the actual mechanism is a physical degradation process driven by the aggressive plasticization of the amine-cured epoxy thermoset matrix as the diffusing ionic species binds with the polar moieties and disrupts the noncovalent bonding within the polymer network. The ensuing nonequilibrium swelling behavior led to physical erosion, which was observed to be the main degradation mechanism. Understanding how the diffusion of acidic electrolyte into thermoset matrix leads to a corresponding degradation in material properties[8,9] or erosion would facilitate the educated selection of suitable materials and assist in the molecular design of tailormade resin precursors for either applications requiring improved chemical resistance or even controlled chemical degradation of the thermoset resin matrix to enable composite fiber recovery[5,10] and polymer recycling.[1,2]

Recent interest in the diffusion of acids in polymers is related to understanding the mechanism behind the resolution limitation of chemical amplified photoresists to enable the design of more precise materials for nanoelectronics.[11,12] Even though many contemporary works were reported on the topic of acid-degradable thermoset for sustainable polymer chemistry, these research studies focused on the acid-degradable polymer chemistry and largely ignored the acid diffusion mechanic studies.[1−4] Thus, in this work, the objective was to understand comprehensively the accelerated diffusion mecha-

Received: March 28, 2019
Accepted: June 10, 2019
Published: June 20, 2019

DOI: 10.1021/acsomega.9b00859
ACS Omega 2019, 4, 10799−10808

nism of acid electrolytes into glassy thermosets and propose explanations for the various phenomena observed leading to eventual material degradation.

Neogi compiled an excellent overview of various phenomena and models related to diffusion into polymers, and while most of the diffusion systems reviewed were thermoplastics, the concepts are expected to hold true for thermoset systems.[13] Hojo et al. presented the classical phenomena of the erosion-corrosion process by which a thermoset undergoes chemical degradation when immersed in corrosive media.[14] A similar mechanism in biodegradable polymers was reported by Göpferich et al., who presented a theoretical model based on the ratio between the penetrant diffusion rate and the polymer degradation rate.[15,16] While these studies focused on the consequential degradation behavior, they provide little insight into the basis behind the rapid diffusion of acidic electrolyte into the thermoset matrix compared with benign media like water.

On the contrary, water diffusion into epoxy thermosets has been studied extensively and the network effects well understood;[9,17−20] however, controversy remains due to the many proposed diffusion theories that have yet to be definitively disproved or established as the dominant mechanism.[21−26] In spite of the debates, recent pieces of evidence point toward the domineering effect of network polarity over other factors such as free volume or cross-link density to influence equilibrium water sorption and the uptake rate.[9,23,26−30] Most of the epoxy-water diffusion systems investigated were able to reach equilibrium sorption, indicating the lack of chemical degradation or erosion observed within the timespan of the studies; however, Toscano et al. utilized a photoelastic stress analysis technique to reveal the evolution of swelling stresses over the period of water sorption.[31] Thus, for systems with a larger mass uptake, it would be expected to undergo erosion by swelling-induced fractures along the swelling stress boundaries. Dielectric studies were used to correlate the relationship between dielectric permittivity and absorbed moisture, as well to identify the bounded state of water within the epoxy matrix,[32−34] which might be useful to monitor the diffusion of more polar electrolytes into the epoxy matrix. Miszczyk et al. further developed methods to correlate impedance data from electrochemical impedance spectroscopy to obtain the corresponding capacitance values that were found to vary with gravimetric data of amine-cured epoxy coatings immersed in water.[35]

The aim of this paper was to describe in detail the sorption behavior of hydrochloric acid (HCl) into an amine-cured epoxy by concurrent gravimetric measurements and dielectric monitoring. The swelling mechanisms leading to eventual physical erosion were investigated by modulated dynamic scanning calorimetry (mDSC) and Fourier transform infrared-attenuated total reflection (FTIR-ATR). The epoxy-amine system was studied in various stoichiometric ratios to briefly address the effect of network polarity and cross-link density in relation to HCl sorption.

THEORETICAL BACKGROUND

Gravimetric Measurements. The one-dimension Fick's diffusion equation can be solved by applying initial and boundary conditions[36] for values of M_t/M_∞ lower than 0.5 to give the following

$$\frac{M_t}{M_\infty} = 4\left(\frac{Dt}{\pi l^2}\right)^{1/2} \quad (1)$$

where M_t is the total amount of penetrant that entered the substrate at time t relative to the initial dry specimen mass, M_∞ is the equilibrium penetrant content after a very long time, l is the substrate thickness, and D is the diffusion coefficient.

D can be calculated from the slope of the M_t versus $t^{1/2}$ curve by rearrangement of eq 1 into the following

$$M_t = (4M_\infty\sqrt{D/\pi})\frac{\sqrt{t}}{l} \quad (2)$$

It must be noted that similar works in the literature may or may not have taken into consideration the effect of the substrate thickness variation due to swelling.[17−21,27−29] While this effect may be considered miniscule and thus negligible in epoxy/water swelling systems, the thickness variation was observed to be quite significant for epoxy/HCl acid swelling systems, which experience upward of 50% mass increase and over 20% thickness increase before fracture. Due to the non-Fickian nature of the epoxy/acid diffusion system and the above-mentioned issue of sample fractures due to non-equilibrium swelling, eq 2 may not be the most suitable equation to model the entire diffusion process. However, after considering the complexity of the acid swelling process, the lack of alternative models, and the insights it delivers compared with the well-studied epoxy/water systems, it was decided that this model is still relevant in spite of its limitations to represent the intrinsic differences of epoxy/acid diffusion systems. As D cannot be directly obtained using eq 2 as the equilibrium mass is unmeasurable due to fractures, the initial linear slope portion of the M_t versus $t^{1/2}$ curve, S_i, is proposed to be a representative diffusion function proportional to D.

$$S_i = 4M_\infty\sqrt{D/\pi} \quad (3)$$

The idealized Fickian diffusion behavior can typically be observed only in lightly cross-linked elastomers above its T_g, as the mechanism of solvent uptake is understood to be dominated by the occupation of free volume sites with minimal interactions between the solvent and the polymer. For most polymer systems that undergo swelling, the diffusional behavior cannot be adequately described by the idealized Fickian theory;[37] thus, eq 1 can be simplified into

$$M_t = kt^n \quad (4)$$

where M_t is the mass uptake, k is a constant, t is the immersion time, and $n = 1/2$ for Fickian behavior. Non-Fickian anomalous diffusion is characterized by $1/2 < n < 1$.

RESULTS AND DISCUSSION

Difference between Water and HCl Diffusion by Gravimetric Measurement. Amine-cured epoxies with different cross-link densities and network polarities were immersed in water and 10 M HCl in an attempt to identify the difference in the diffusion mechanism and to characterize the subsequent thermoset network response.

Diffusion of water into epoxy thermosets has been studied extensively, but there remains uncertainty regarding the effect of free volume or other network interactions such as adsorption and polarity effects; thus, to address this issue, multifunctional amine and epoxy monomers were cured in various amine hydrogen/epoxide ratios (r = 0.5−1.5) to form

DOI: 10.1021/acsomega.9b00859
ACS Omega 2019, 4, 10799−10808

samples ranging from amine-deficient to amine-rich, thus bringing about a diversity of network polarities and cross-link densities to evaluate the diffusion behavior (Table 1).

Table 1. Dielectric and Mechanical Characterization of Amine-Cured Epoxy at Various Amine Hydrogen/Epoxide Equivalent Molar Ratios (r)

	*R*0.5	*R*0.7	*R*0.9	*R*1.0	*R*1.3	*R*1.5
r	0.5	0.7	0.9	1.0	1.3	1.5
T_g (°C)	199	198	210	234	208	192
$E'_{T_g+40°C}$ (MPa)	107	77	160	247	102	64
ρ (g cm^{-3})	1.27	1.30	1.25	1.24	1.24	1.22
M_C	0.15	0.21	0.10	0.06	0.15	0.24
k (1 kHz)	3.67	4.41	3.48	3.98	3.45	3.76

Interesting to note, while it was predicted that the dielectric constant is indicative of the network polarity and thus proportional to the amine content of the amine-cured epoxy samples, this relationship was not observed in the obtained dielectric constant results. The cross-link density result did not exactly comply proportionally with the projected cross-link density from stoichiometric predictions. The deviations from prediction were proposed to be due to the formation of specific, thermodynamically preferable oligomeric conformations during the initial cure process, which result in the excess end group moieties being frozen in place during subsequent vitrification, thus leading to the observed deviation in network polarity and cross-link density from stoichiometric predictions. Nonetheless, the variation in material characteristics of the various amine hydrogen/epoxide ratios (r = 0.5−1.5) suffices for this study to investigate the effects on diffusion behavior in both water and concentrated HCl. The results of water diffusion were then compared to the diffusion study of amine-cured epoxy in 10 M HCl to identify the different mass uptake characteristics and phenomena.

The mass uptake behavior of epoxies in water (Figure 1A) was observed to be in agreement with that of other studies,[23,27] in that water diffuses more readily into networks with a higher amine content (larger r value) and reaches a higher equilibrium mass. The influence of free volume, which was theoretically dependent on density and cross-link density, did not appear to influence the mass uptake or equilibrium mass at all with regard to water diffusion. The mass uptake rate in 10 M HCl (Figure 1B), as represented by the obtained S_i value, was observed to be over an order of magnitude higher compared with that of water. No equilibrium mass was observed in 10 M HCl due to eventual physical erosion and disintegration before equilibrium could be reached. Again, networks with higher amine content were observed to absorb HCl faster and physically disintegrate within a short immersion time. Sample *R*0.9 with a higher cross-link density was observed to maintain physical integrity and achieve the highest mass uptake before disintegration than the rest. These results indicate that while the diffusion rate is dependent on network polarity, the cross-link density also plays an important role in maintaining physical integrity, especially for systems that experience significant swelling. The results were observed to be in agreement with the study by Li et al.,[23] in that the binding with polar amine sites within the thermoset network is an essential factor determining the equilibrium mass for both water and HCl, but the achievable equilibrium mass was also found to be limited by mechanical constraints before physical degradation occurs.

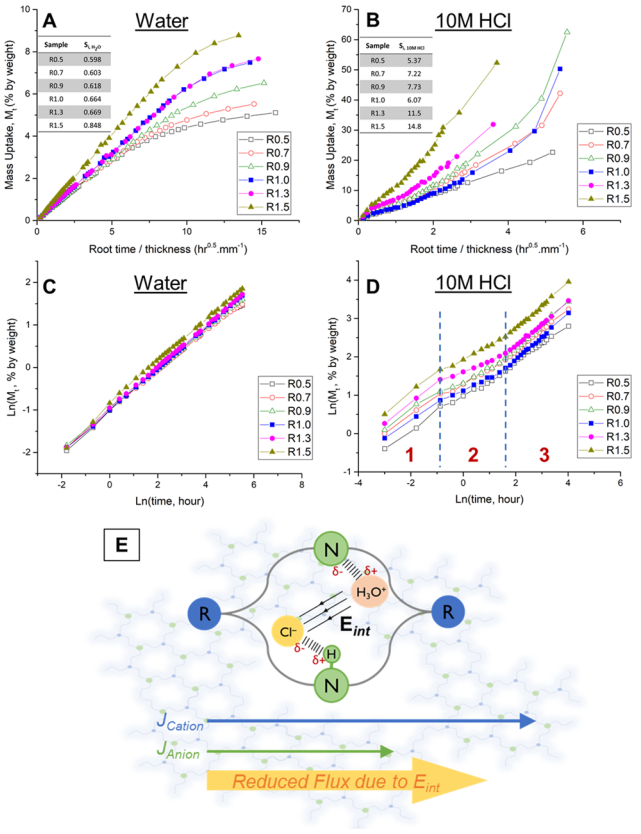

Figure 1. Mass uptake curve of amine-cured epoxies in (A) water and in (B) 10 M HCl; the diffusion rate of HCl into epoxy was observed to be an order of magnitude faster compared with that of water. Diffusion behavior of amine-cured epoxies in (C) water, which is Fickian-like, and in (D) 10 M HCl, where a 3-stage diffusion mechanism of HCl into epoxy was observed. (E) The formation of E_{int} restricts the flux of the faster diffusing cationic species, leading to the 3-stage diffusion mechanism.

The diffusion behavior was evaluated according to eq 4. Water diffusion (Figure 1C) was observed to adhere closely to the Fickian diffusion behavior with $n \approx 0.5$ at various r values, indicating that while the network polarity and cross-link density were expected to influence the diffusion coefficient, they did not affect the diffusion behavior as the thermoset remains glassy until equilibrium mass was reached. Conversely, the diffusion behavior of HCl was observed to follow a 3-stage mechanism, followed by eventual physical disintegration before equilibrium mass was achieved (Figure 1D).

On first impression, it was proposed that the 3-stage HCl diffusion mechanism was due to erosion of the samples under excessive swelling. However, the erosion of samples was only observed after some periods of swelling, and different samples begin eroding at different times; thus, while the erosion phenomenon was observed, it was not likely to cause the 3-stage HCl diffusion mechanism. Furthermore, in spite of the different network polarity and cross-link density of the amine-cured epoxy samples, the three stages were observed to occur within the same time phase, indicating that the mechanism should be due to the specific diffusion behavior of the HCl acid electrolyte instead of the thermoset matrix characteristics.

It was proposed by Zaikov et al. that the diffusion of the electrolytes into polymers should take into consideration the

DOI: 10.1021/acsomega.9b00859
ACS Omega 2019, 4, 10799−10808

diffusivity of individual ionic components of the electrolyte media instead of simply assuming the diffusion of the electrolyte as a homogeneous penetrant.[9,38] Consequently, the different diffusivities of cationic and anionic penetrants into the polymer bulk would lead to the formation of an interior electric field (E_{int}) between the cationic and anionic propagation fronts. The E_{int} would restrict the diffusivity of the ionic species, subsequently resulting in reduced diffusivity of the ionic species, as observed in stage II of HCl diffusion. Eventually, an equilibrium would be reached between the diffusion of ionic species driven by the concentration gradient and the restrictive E_{int}, resuming diffusive propagation as a unified layer at stage III of HCl diffusion (Figure 1E). Thus, the 3-stage mechanism of HCl acid electrolyte behavior appears to be in agreement with the theoretical proposition made by Zaikov et al. over 30 years ago.

The obtained cross-link density in Table 1 infers the covalent network density as the M_c is obtained from the rubbery modulus at $T_{g+40°C}$. Thus, the cross-link density would not have much of an effect on E_{int}, which is dependent on the electrostatic interactions between the bounded ionic species. As observed from the mass uptake curves of *R*0.5−1.5 (Figure 1B), the diffusivity was found to be determined by the concentration of polar amine species (secondary and tertiary amine), instead of the expected covalent cross-link density. The ability of the amine moieties to attract ionic acid penetrants overshadows the restriction of network relaxation as imposed by the cross-link density.

To summarize, cross-link density does not appear to have any effect on E_{int} or diffusion of ionic penetrants.

Effect of HCl Concentration on Swelling Behavior. As *R*0.9 was observed to tolerate the largest swelling in HCl, it was used to study the effect of HCl concentration on mechanisms of physical degradation during acid swelling. Interesting point to note, HCl acid with concentration above 25 wt % (~8 M) is classified as corrosive liquid, whereas it is only considered an irritant at concentrations below 25 wt %. Thus, while no formal research has been performed to determine the diffusion mechanism of HCl acids into polymers, industrial experience and qualitative studies indicated the influence of HCl concentration on acid diffusion into the polymer matrix. As expected, increasing HCl concentration corresponds to an increase in the mass uptake rate (Figure 2). During the course of study, it was observed that at high HCl concentration above 8 M, *R*0.9 experienced core−shell swelling, leading to rapid disintegration due to swelling stresses and eventual erosion of the surface. The concurrent erosion mechanism while swelling complicates the mass uptake measurements, as only the net weight gain could be recorded. Thus, although the reported net mass uptake values for 8 and 10 M appear to be lower than 5 M, it is in truth much higher due to the erosion loss. The higher acid concentration would lead to a higher concentration gradient between the surface and the interior bulk, thus leading to higher diffusivity. The surface erosion phenomenon, while being attributed to the swelling-induced physical degradation that is dependent on diffusivity, is also dependent on the available surface area. The mass uptake values for 10 M HCl concentration appeared to be double that of 8 M, as the epoxy specimen swells much more with a thicker swollen shell than 8 M, but the erosion rate was only slightly higher due to a limited surface area available for erosion. It must be noted that even with crazes and cracks, the fractured but-yet-to-be eroded surface still experiences significant swelling that contributes to

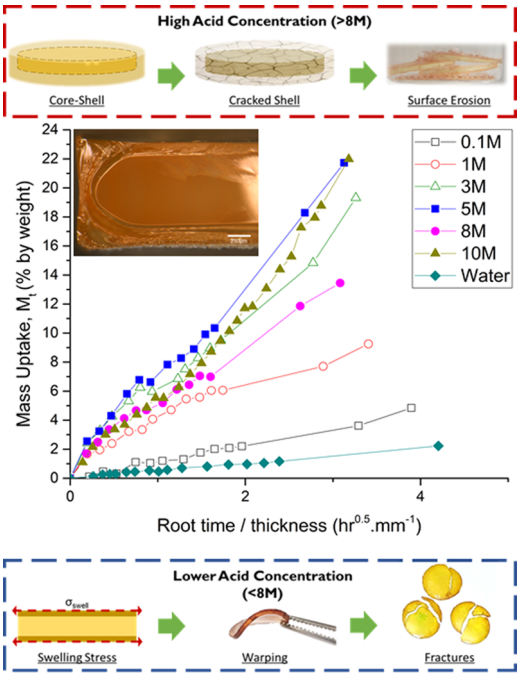

Figure 2. Mass uptake of *R*0.9 at HCl concentration from 0.1 to 10 M, and the physical degradation mechanism observed. The mass uptake rate of *R*0.9 in 8 M and 10 M HCl appeared to be lower than that of 5 M due to surface erosion loss during measurement. In general, mass uptake increases correspondingly with HCl concentration. The inset shows the cross-section micrograph of *R*0.9 in 10 M HCl after 24 h when core−shell swelling is evident.

the observed mass uptake. Whereas at lower HCl concentration (<8 M), although the diffusion of HCl into amine-cured epoxy appeared to be relatively stable with little erosion loss, the significant swelling of the exterior layers led to formation of stress gradients, which cause warpage and eventual fracture of the sample disks after prolonged swelling (refer to Supporting Information S4).

Core−shell swelling has previously been reported in various polymer systems[14−16,37] and was described in detail by C.E. Rogers as Case II diffusion in which the diffusion was observed to be so rapid that a distinct boundary was observed between the swollen exterior and the glassy inner core. In the case of *R*0.9 immersed in HCl larger than 8 M, the rapidly swollen exterior was observed to be only a thin surface layer, which cracked and eroded away from the unswollen bulk. Even when core−shell swelling behavior was not observed, the evolution of strained layers in the exterior due to swelling-induced stress transfer to the unswollen core was reported to influence the penetrant diffusion rate.[39] Thus, when also taking into consideration the electric field restricted electrolyte diffusion and the thermophysical changes of the polymer matrix due to plasticization effects, it would present a highly complicated challenge to model the acid diffusion process in light of so many variables and concurrent processes.

Dielectric Changes during HCl Uptake. To validate the theory of electric field restricted diffusion and investigate the noncovalent polar binding interactions between the diffusing HCl species and the amine-cured epoxy matrix, dielectric measurements were performed concurrently with weight monitoring when *R*0.9 was immersed in deionized water and 10 M HCl at 60 °C. The dielectric constant measured at 1 kHz

DOI: 10.1021/acsomega.9b00859
ACS Omega 2019, 4, 10799−10808

is indicative of the ionic polarization response when the penetrant diffuses into the amine-cured epoxy network.

The obtained result for dielectric response of diffused water into *R*0.9 (Figure 3A) was observed to be consistent with that by Garden et al. on dielectric changes due to water diffusion in another epoxy system, in that the increase in dielectric constant does not correspond proportionally to the increase in water uptake mass, which was explained by a network confinement effect restricting the dipolar response.[32] In contrast, the measured dielectric constant was found to increase accordingly with HCl mass uptake over time (Figure 3B), and a sharp increase in the dielectric constant by a few orders of magnitude was observed after the onset of HCl diffusion stage II. Initially, it was proposed that the onset of stage II during electrolyte diffusion was due to the restriction of ionic mobility to maintain charge neutrality;[9,38] however, the exceptionally large increase in dielectric constant up to almost 5000 cannot be explained without also taking into consideration the effects of polar interactions with the matrix. For comparison, the dielectric constant of *R*0.9 was measured to be about 3.5 initially, 10 M HCl was measured to be around 5, and water was around 80. Thus, the large dielectric constant could only be explained by the ionic polarization between HCl and the tertiary amine moieties within the amine-cured epoxy network, which stabilizes the charge separation between the electrolyte ionic species and thus contributes to the large increase in the measured dielectric constant. The exceptionally large dielectric constant was only observed at relatively low frequencies, which corresponds to ionic polarization, and the effect disappears at higher frequencies, further confirming the phenomenon to be due to the charge separation effects caused by the polar interactions between HCl ionic species and the amine-cured epoxy network (Figure 3D). Water does not disassociate in the epoxy network (Figure 3C); thus, while the slight increase in dielectric constant could be attributed to the interaction with polar moieties such as hydroxy and amine functionalities,[32] no significant increase in dielectric constant similar to HCl swelling was observed. The formation of E_{int} is only possible in the heavily plasticized, swollen state, whereby the ionic acid penetrants completely bind to the polar network moieties and

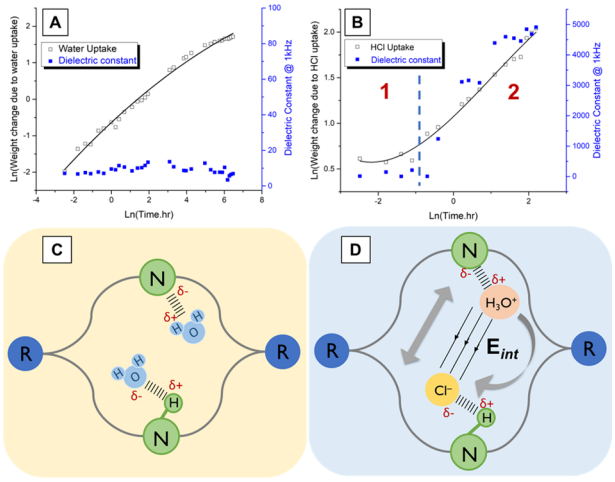

Figure 3. Mass uptake of (A) water and (B) HCl into amine-cured epoxy *R*0.9 with concurrent dielectric constant measurement at 1 kHz. Schematic of the proposed interaction between the epoxy network and either (C) water or (D) HCl. The significant increase in the dielectric constant at the onset of the stage 2 HCl diffusion mechanism is due to ionic polarization contribution by E_{int} formed when polar HCl ionic species interact with the tertiary amine moieties and partially disassociate within the amine-cured epoxy network. Water does not disassociate in the epoxy network; thus, no significant increase in the dielectric constant was observed.

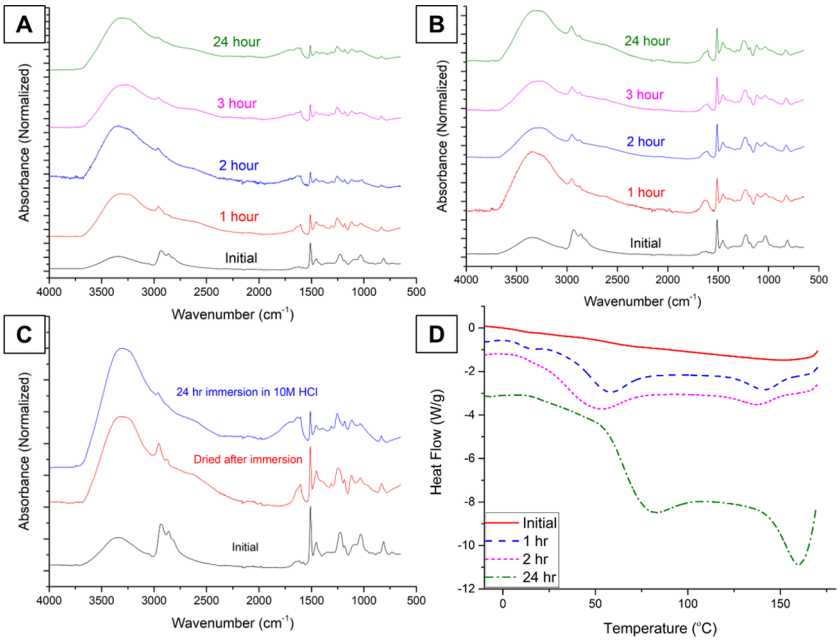

Figure 4. (A) FTIR-ATR monitoring of *R*0.9 immersed in 10 M HCl for up to 24 h. (B) FTIR-ATR analysis of oven-dried samples of *R*0.9 after immersion in 10 M HCl. (C) Comparison of FTIR-ATR spectra of *R*0.9 before and after immersion in 10 M HCl for 24 h. No notable chemical degradation of the epoxy network by HCl was observed due to the unchanged spectra in the fingerprint region. (D) mDSC analysis of the HCl desorption endotherm after *R*0.9 immersion in 10 M HCl indicates the presence of 2 distinct binding states between HCl and the amine-cured epoxy network.

DOI: 10.1021/acsomega.9b00859
ACS Omega 2019, 4, 10799−10808

thus replace the polar/hydrogen bonding network with a polyelectrolyte-like network as described by E_{int}. Thus, E_{int} is an indication that the heavily plasticized, swollen state has been reached, at least in the outer shell regions. The subsequent swelling-induced physical degradation occurs due to the stress-relief mechanisms of crazes and cracking, which lead to surface erosion. Even when there is no core−shell swelling observed as in the case of HCl concentration <5 M, swelling and associated plasticization still occur throughout the epoxy specimen with a more gradual concentration gradient. E_{int} still exists, but the magnitude of the dielectric contribution is lower due to a lower degree of plasticization, which corresponds to a lower degree of network relaxation. A comparison between the dielectric response with mass uptake for epoxy in 3 M and 10 M HCl is included in the Supporting Information S9.

Changes in Surface Morphology due to Swelling during HCl Uptake. Optical monitoring of acid diffusion and reaction with cured epoxies could be performed with in situ UV−vis spectroscopy[40] and micro-ATR/FTIR,[41] and often the objective was to obtain information related to the kinetics of acid reaction with the epoxy matrix. Kinetics of acid diffusion into cured epoxies systems could not be performed by FTIR techniques due to the strong, broad absorbance of acids in the 3500−3000 cm^{-1} range. FTIR analysis in the transmission mode tends to yield little information due to spectra saturation. Instead, a surface characterization technique like FTIR-ATR was performed to evaluate the physiochemical response of the epoxy exterior when immersed in 10 M HCl acid. This technique is especially useful to evaluate the characteristics of the swollen exterior layers due to core−shell swelling. Sample disks of *R*0.9 were immersed in 10 M HCl at 60 °C and removed after 1, 2, 3, and 24 h and immediately analyzed by FTIR-ATR. The sample disks were subsequently dried in an oven at 180 °C for 1 h and then analyzed again by FTIR-ATR to evaluate if HCl is physically adsorbed or covalently reacted with the epoxy matrix.

The absorbance peak at 1510 cm^{-1} attributed to the stretching mode of the aromatic ring in the epoxy monomer was identified as the invariant band. During immersion in 10 M HCl (Figure 4A), the broad peaks corresponding to −OH and −NH bands in the 3500−3200 cm^{-1} region were observed to increase significantly in intensity with respect to the invariant peak at 1510 cm^{-1} over time, attributed to the contribution by adsorbed HCl hydrates within the amine-cured epoxy matrix. Furthermore, it could be observed that while the initial −OH peak was centered at 3350 cm^{-1}, another peak at 3250 cm^{-1} emerged after HCl immersion, leading to formation of a plateaulike broad peak, which could be attributed to the ionic bonding between HCl and tertiary amine moieties within the epoxy network to form an ammonium chloride salt complex. The formation of salts disrupts the noncovalent polar interactions within the amine-cured epoxy matrix and facilitates further plasticization by HCl, leading to the anomalous diffusion behavior and the core−shell swelling as observed. After the HCl was dried off by heating in an oven (Figure 4B), no significant deviation was observed in the fingerprint region from 1500 to 650 cm^{-1}, indicating that very little degradation could be attributed to chain scission events due to acid-catalyzed hydrolytic degradation of ether and amide linkages. Instead, the broad plateau attributed to HCl hydrates and ammonium chloride salt complex remains despite being lower in intensity, evident of the strong binding between HCl and tertiary amine moieties. A further comparison between the initial *R*0.9 before immersion, after immersion in 10 M HCl for 24 h, and after further oven-drying has shown that other than the polar interactions indicated by the broad peak 3500−3200 cm^{-1} region as explained earlier, no significant chemical degradation reactions were observed (Figure 4C); thus, it can be concluded that the HCl acid degradation of this amine-cured epoxy system proceeds via a physical degradation mechanism due to swelling stress.

Water is known to exist in bounded and unbounded states within amine-cured epoxy networks, based on dielectric studies,[34] diffusion studies,[18,42] and thermogravimetric analysis.[43] Instead, modulated DSC was presented in this work as another technique to concurrently evaluate the binding states of adsorbed HCl and the extent of plasticization of the epoxy matrix by adsorbed HCl. Again, *R*0.9 was immersed in 10 M HCl at 60 °C for 1, 2, and 24 h; then, the sample was removed, wiped dry, and immediately crimped within hematic aluminum pans for mDSC heating and cooling run cycles. The desorption endotherm (Figure 4D) indicated that the adsorbed HCl within the epoxy matrix exists in either unbounded or bounded states due to the presence of two distinct endotherms, namely, below and above the boiling point of water. The unbounded state refers to the adsorbed HCl hydrates within the free volume of the swollen epoxy, as it would be rapidly removed upon thermal removal of water as outgassing HCl. The bounded state corresponds to the ammonium chloride salt complex previously described by the FTIR-ATR study. As the HCl desorption endotherm was observed to be broad and shifts toward higher temperatures over prolonged immersion in 10 M HCl, the adsorbed and bounded states do not appear to be a distinct state but rather occur as a complex distribution of bounded states due to the amorphous nature of the amine-cured epoxy network morphology. The shift of the endotherms toward higher temperature is due to the increase in thermal stability of the adsorbed HCl due to lower entropy as the acid/epoxy diffusion system approaches thermodynamic equilibrium. Furthermore, the adsorbed HCl would increase the heat capacity of the system by increasing the chain mobility of the amorphous network, whereas after desorption, the system returns to its glassy amorphous state. Therefore, the difference in heat capacity measured during heating and cooling cycles could be used to compare the degree of plasticization of the acid/epoxy system (Table 2). In general, longer immersion time corresponds to more significant swelling and a higher degree of plasticization, and the mDSC is a suitable technique to monitor such changes.

Table 2. Heat Capacity of *R*0.9 before and after HCl Desorption, Measured by mDSC

	initial	1 h	2 h	24 h
$C_{60°C,heating}$	1.76	1.461	1.607	1.532
$C_{60°C,cooling}$	1.681	1.347	1.306	1.123
$\Delta C_{60°C}$	0.079	0.114	0.301	0.409

To verify and visualize the physical degradation resulting from the proposed swelling stress-induced cracks and the erosion mechanism, an electron micrograph was obtained from vacuum-dried sample disks of *R*0.9 immersed in 10 M HCl at 60 °C for 2, 4, and 7 h (Figure 5). The initial amine-cured epoxy surface can be considered relatively smooth and homogeneous (Figure 5A); the particles observed on the

DOI: 10.1021/acsomega.9b00859
ACS Omega 2019, 4, 10799−10808

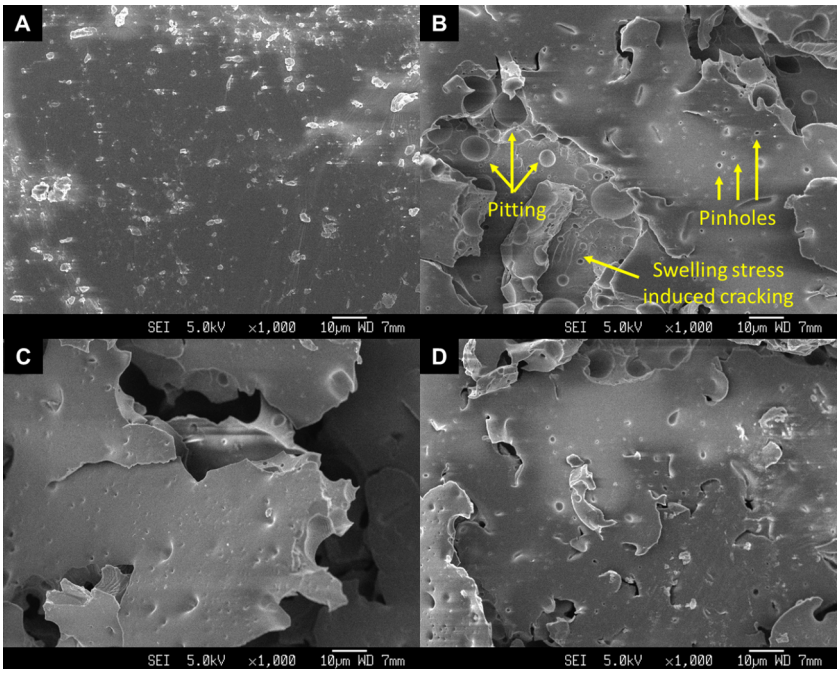

Figure 5. Field emission scanning electron microscopy (FESEM) micrograph of the *R*0.9 sample surface before (A) and after immersion in 10 M HCl for 2 h (B), 4 h (C), and 7 h (D). Physical degradation proceeds by (B) swelling-induced surface crack formation, (C) crack propagation leading to exterior delamination, and (D) repetition of crack formation and delamination leading to the observed surface erosion mechanism.

surface can be attributed to dust residues, which settled on the epoxy during the casting process and is unlikely to affect the subsequent acid degradation mechanism. After immersing in 10 M HCl for 2 h (Figure 5B), one can observe cracks, pinholes, and pits on the specimen surface. It is important to note that the captured electron micrograph is representative of the deswollen exterior surface after vacuum-drying to remove HCl hydrates due to its tendency to outgas.

First, the proposed mechanism behind the formation of pinholes can be attributed to the chemical attack by HCl on the unreacted resin precursors or partially reacted clusters within the amine-cured epoxy network. These clusters that are susceptible to HCl acid attack were formed due to the vitrification of the entire network, which impedes the subsequent diffusion of unreacted species from achieving reaction completion. The formation of pits as observed might be caused by the formation of HCl gas pockets from the unbounded HCl hydrates during the drying procedure of sample preparation for FESEM imaging. Similar pits were previously observed in injection molded ABS samples and were attributed to volatile outgassing during molding.[44] The pits were mostly observed to form at the layer below the delaminated exterior, which supports the theory that such pits are likely to be artifacts from sample preparation for FESEM imaging. Lastly, the cracks did not appear to originate from any specific defect sites and were distributed homogeneously throughout the specimen surface. It was also obvious that the cracks propagated beneath the exterior layers and resulted in the delamination of the surface from the bulk. The only reasonable explanation was that the crack propagated along the interface between the swollen exterior and the unswollen interior bulk. As observed by the change in specimen surface degradation over a period of immersion time, it appeared that the physical degradation occurred in cyclic repetition between the exterior swelling (Figure 5B) followed by exterior delamination (Figure 5C) and again (Figure 5D), leading to the observed surface erosion phenomena. While this proposed mechanism may appear to be similar to environmental stress cracking of polymers, the key difference in this mechanism is that the origin of the stress source is contributed by the swelling stress and not an externally applied stress.

CONCLUSIONS

Herein this work, a diffusion study of amine-cured epoxy in concentrated HCl was presented to unravel the mechanistic origins of the observed physical degradation phenomena that were presumptuously attributed to chemical degradation reactions previously. Through concurrent gravimetric and dielectric monitoring, it was revealed that the diffusion mechanism of HCl into amine-cured epoxy networks turns out to be contrastingly different from that of the well-studied water/epoxy diffusion systems. The partial dissociation of acid electrolyte within the epoxy network led to the observation of an anomalous 3-stage diffusion mechanism, which was also characterized by the concurrent sharp increase in the dielectric constant of the HCl-swollen epoxy system due to the formation of E_{int}. Further evidence that supports the swelling-induced physical degradation as the dominant degradation mechanism was indicated by the lack of chemical changes within the fingerprint region of the FTIR spectra over the HCl swelling duration, as well as the observed desorption of bounded and unbounded HCl from the swollen epoxy matrix. Electron micrographs of the dried epoxy specimen surfaces over a period of HCl swelling have shown characteristic features of environment stress cracking of polymers, which was attributed to the complementary action of the swelling-induced stress due to the large mass uptake, with the plasticizing effect of acid on the epoxy network leading to the erosion-type degradation mechanism observed.

DOI: 10.1021/acsomega.9b00859
ACS Omega 2019, 4, 10799−10808

Thus, the proposed epoxy/acid degradation mechanism based on the failure analysis insights does not appear to be restricted to either this specific epoxy system or the HCl media. Instead, the degradation mechanisms could be generally applied to the diffusion or degradation studies of a polar thermoset matrix immersed in concentrated electrolytes. Therefore, specialty solvents could be designed to harness the presented accelerated diffusion mechanism for faster, higher-yielding thermoset disintegration processes to enable thermoset recycling or composite fiber recovery applications. The large dielectric response could also be used to develop in situ sensors utilizing dielectric constant measurements with cheap handheld LCR meters to monitor the safe usage lifetime of thermoset composites used in corrosive environments.

EXPERIMENTAL SECTION

Materials. *N*,*N*-Diglycidyl-4-glycidyloxyaniline, alternatively known as triglycidyl-*p*-aminophenol (TGAP) epoxy resin, with epoxide equivalent 100 g mol^{-1} was obtained from Sigma-Aldrich. Bis(aminomethyl)norbornane (NBDA) with amine hydrogen equivalent 38.5 g mol^{-1} was obtained from Tokyo Chemical Industry. The liquid resin precursors were used as received. Hydrochloric acid (37%) was obtained from Merck and diluted to the respective concentrations (0.1−10 M) with deionized water generated in our laboratory.

Sample Preparation. The epoxy samples were prepared by mixing TGAP and NBDA according to predefined amine hydrogen/epoxide equivalent molar ratios (r) of 0.5, 0.7, 0.9, 1.0, 1.3, and 1.5, to vary the network polarity and cross-link density. The mixtures were subsequently degassed by centrifuge and cast in silicon molds with 1.27 cm-diameter disc cavities with depth of 2 mm. The samples were cured at 25 °C for 12 h, followed by postcuring at 120 °C for 2 h. The cured sample disks were stored in dehumidifier cabinets and preconditioned by overnight drying in a vacuum oven at 80 °C prior to testing (Figure 6).

Gravimetric Measurements with Dielectric Monitoring (Figure 6). Acid sorption studies were performed by immersing the sample disks in hydrochloric acid of various concentrations at 60 °C. The samples were periodically removed from the acid, quenched in deionized water twice, gently patted dry on filter paper, and immediately measured. The sample disc thickness was measured by a Mitutoyo digital micrometer screw gauge with precision of 0.001 mm and then weighed with an A&D GR-202 semimicro balance with precision of 0.01 mg. Three samples were measured for each sample set. Subsequently, one sample was selected out of each set for measurement of its dielectric properties using a Keysight E4980A LCR meter equipped with ASTM D150-compliant dielectric test fixture 16451B. The dielectric test fixture based on a parallel-plate design with gold-coated stainless steel electrodes was cleaned with acetone before and after every measurement to remove residues. A reference HDPE film sample was measured periodically to ensure the equipment was within calibrated limits. The samples were monitored until large fractures occurred. The experiment was performed entirely within a fumehood due to the outgassing of HCl gas from the acid swollen specimens during measurements.

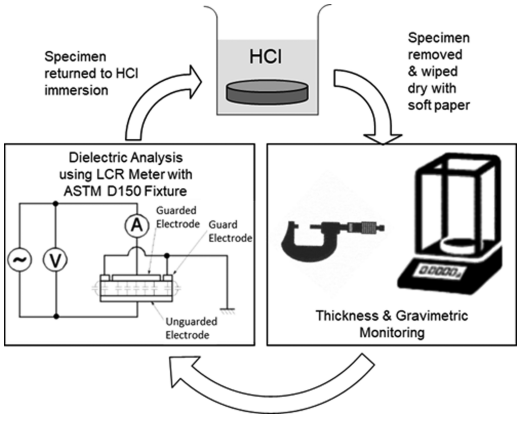

Figure 6. Schematic of the experiment workflow, starting with specimen immersion in HCl for a specified duration, followed immediately by thickness, mass measurements, and dielectric analysis.[45] The specimen was returned to HCl immersion, and the monitoring cycle was repeated until disintegration.

Other Characterizations. Dynamic mechanical analysis was performed with TA instruments Q800 DMA utilizing the single cantilever mode with temperature ramp from ambient to 300 °C to estimate the molecular weight between cross-links in accordance with the rubber elasticity theory[46] using the storage modulus value at T_g + 40 °C according to the following equation

$$M_c = 3RT\rho/E'_{T_g+40^\circ C} \quad (5)$$

Density measurements were performed using an Ultrapyc 1200e helium gas pycnometer by Quantachrome instruments.

Modulated dynamic scanning calorimetry (mDSC) was performed using TA 2920 mDSC with aluminum pans under dry nitrogen gas. The samples were equilibrated at −20 °C, then heated at 10 °C min^{-1} with temperature modulation of 1.6 °C min^{-1} up to 180 °C, followed by controlled cooling at 10 °C min^{-1} with temperature modulation of 1.6 °C min^{-1} until −20 °C. This technique was able to identify different types of bonding between the adsorbed HCl and the epoxy network, as well as a guide to determine the degree of plasticization of the epoxy network based on the difference in measured heat capacity between the heating and cooling cycles.

FTIR-ATR was performed using Perkin Elmer Frontier in the mid-IR range with diamond ATR accessory from 4000 to 650 cm^{-1}. ATR correction was performed using the algorithm included with the accompanying Spectrum software platform to reduce spectra distortion. This technique was performed on samples before and after drying to understand the chemical interactions within the epoxy network at different immersion times.

Secondary electron micrograph was obtained using JEOL JSM-6340F with a cold-field-emission source at an accelerating voltage of 5 kV and working distance of 7 mm. The acid-immersed samples for imaging were prepared by quenching twice with deionized water, followed by reduced-pressure-drying in a vacuum oven at 80 °C and −28.8 in Hg. The samples were coated with platinum prior to imaging.

ASSOCIATED CONTENT

Supporting Information

The Supporting Information is available free of charge on the ACS Publications website at DOI: 10.1021/acsomega.9b00859.

DOI: 10.1021/acsomega.9b00859
ACS Omega 2019, 4, 10799−10808

Calculations involved in sample preparation, results to supplement the M_c calculations, photos showing sample disintegration behavior, heat capacity results from mDSC, and dielectric constant monitoring data over the duration of 10 M HCl immersion with explanation, discussions involving the effects of acid concentration on diffusion behavior and dielectric constant, core−shell swelling stress fields (PDF)

AUTHOR INFORMATION

Corresponding Authors

*E-mail: Jacoblim@ntu.edu.sg (J.S.K.L.).
*E-mail: ASXHU@ntu.edu.sg (X.M.H.).

ORCID

Jacob Song Kiat Lim: 0000-0002-8009-7425

Notes

The authors declare no competing financial interest.

ACKNOWLEDGMENTS

This paper was supported by Temasek Laboratories@NTU and School of Materials Science and Engineering, Nanyang Technological University, Singapore.

REFERENCES

(1) Fortman, D. J.; Brutman, J. P.; De Hoe, G. X.; Snyder, R. L.; Dichtel, W. R.; Hillmyer, M. A. Approaches to Sustainable and Continually Recyclable Cross-Linked Polymers. *ACS Sustainable Chem. Eng.* **2018**, *6*, 11145−11159.

(2) García, J. M.; Jones, G. O.; Virwani, K.; McCloskey, B. D.; Boday, D. J.; ter Huurne, G. M.; Horn, H. W.; Coady, D. J.; Bintaleb, A. M.; Alabdulrahman, A. M. S.; Alsewailem, F.; Almegren, H. A. A.; Hedrick, J. L. Recyclable, Strong Thermosets and Organogels via Paraformaldehyde Condensation with Diamines. *Science* **2014**, *344*, 732−735.

(3) Snyder, R. L.; Fortman, D. J.; De Hoe, G. X.; Hillmyer, M. A.; Dichtel, W. R. Reprocessable Acid-Degradable Polycarbonate Vitrimers. *Macromolecules* **2018**, *51*, 389−397.

(4) You, S.; Ma, S.; Dai, J.; Jia, Z.; Liu, X.; Zhu, J. Hexahydro-s-triazine: A Trial for Acid-Degradable Epoxy Resins with High Performance. *ACS Sustainable Chem. Eng.* **2017**, *5*, 4683−4689.

(5) Wang, Y.; Cui, X.; Ge, H.; Yang, Y.; Wang, Y.; Zhang, C.; Li, J.; Deng, T.; Qin, Z.; Hou, X. Chemical Recycling of Carbon Fiber Reinforced Epoxy Resin Composites via Selective Cleavage of the Carbon−Nitrogen Bond. *ACS Sustainable Chem. Eng.* **2015**, *3*, 3332−3337.

(6) De Renzo, D. J. *Corrosion Resistant Materials Handbook*; Noyes Data Corporation, 1985.

(7) Schweitzer, P. A. *Corrosion Resistance Tables: ACE-CHR*; M. Dekker, 2004.

(8) Alessi, S.; Di Filippo, M.; Pitarresi, G.; Scafidi, M.; Toscano, A. Fracture Toughness of Hydrothermally Aged Epoxy Systems with Different Crosslink Density. *Procedia Eng.* **2015**, *109*, 507−516.

(9) Zaikov, G. E. Diffusion and Sorption of Aqueous Electrolyte Solutions in Polymers. *Russ. Chem. Rev.* **1985**, *54*, 885.

(10) Møller, V. B.; Dam-Johansen, K.; Frankær, S. M.; Kiil, S. Acid-resistant organic coatings for the chemical industry: a review. *J. Coat. Technol. Res.* **2017**, *14*, 279−306.

(11) Rodríguez-Cantó, P. J.; Nickel, U.; Abargues, R. Understanding Acid Reaction and Diffusion in Chemically Amplified Photoresists: An Approach at the Molecular Level. *J. Phys. Chem. C* **2011**, *115*, 20367−20374.

(12) Mack, C. A. Lithographic Effects of Acid Diffusion in Chemically Amplified Resists. In *Microelectronics Technology*; American Chemical Society, 1995; Vol. *614*, pp 56−68.

(13) Neogi, P. *Diffusion in Polymers*; Taylor & Francis, 1996.

(14) Hojo, H.; Tsuda, K.; Kubouchi, M.; Kim, D.-S. Corrosion of plastics and composites in chemical environments. *Met. Mater.* **1998**, *4*, 1191−1197.

(15) Göpferich, A. Mechanisms of polymer degradation and erosion. *Biomaterials* **1996**, *17*, 103−114.

(16) von Burkersroda, F.; Schedl, L.; Göpferich, A. Why degradable polymers undergo surface erosion or bulk erosion. *Biomaterials* **2002**, *23*, 4221−4231.

(17) Li, L.; Zhang, S.; Chen, Y.; Liu, M.; Ding, Y.; Luo, X.; Pu, Z.; Zhou, W.; Li, S. Water Transportation in Epoxy Resin. *Chem. Mater.* **2005**, *17*, 839−845.

(18) Zhou, J.; Lucas, J. P. Hygrothermal effects of epoxy resin. Part I: the nature of water in epoxy. *Polymer* **1999**, *40*, 5505−5512.

(19) Nogueira, P.; Ramírez, C.; Torres, A.; Abad, M. J.; Cano, J.; López, J.; López-Bueno, I.; Barral, L. Effect of water sorption on the structure and mechanical properties of an epoxy resin system. *J. Appl. Polym. Sci.* **2001**, *80*, 71−80.

(20) Linde, E.; Giron, N. H.; Celina, M. C. Water diffusion with temperature enabling predictions for sorption and transport behavior in thermoset materials. *Polymer* **2018**, *153*, 653−667.

(21) Frank, K.; Wiggins, J. Effect of stoichiometry and cure prescription on fluid ingress in epoxy networks. *J. Appl. Polym. Sci.* **2013**, *130*, 264−276.

(22) Jackson, M.; Kaushik, M.; Nazarenko, S.; Ward, S.; Maskell, R.; Wiggins, J. Effect of free volume hole-size on fluid ingress of glassy epoxy networks. *Polymer* **2011**, *52*, 4528−4535.

(23) Li, L.; Yu, Y.; Wu, Q.; Zhan, G.; Li, S. Effect of chemical structure on the water sorption of amine-cured epoxy resins. *Corros. Sci.* **2009**, *51*, 3000−3006.

(24) Vanlandingham, M. R.; Eduljee, R. F.; Gillespie, J. W. Moisture diffusion in epoxy systems. *J. Appl. Polym. Sci.* **1999**, *71*, 787−798.

(25) Soles, C. L.; Yee, A. F. A discussion of the molecular mechanisms of moisture transport in epoxy resins. *J. Polym. Sci., Part B: Polym. Phys.* **2000**, *38*, 792−802.

(26) Carter, H. G.; Kibler, K. G. Langmuir-Type Model for Anomalous Moisture Diffusion In Composite Resins. *J. Compos. Mater.* **1978**, *12*, 118−131.

(27) Wang, J.; Gong, J.; Gong, Z.; Yan, X.; Wang, B.; Wu, Q.; Li, S. Effect of curing agent polarity on water absorption and free volume in epoxy resin studied by PALS. *Nucl. Instrum. Methods Phys. Res., Sect. B* **2010**, *268*, 2355−2361.

(28) Merdas, I.; Tcharkhtchi, A.; Thominette, F.; Verdu, J.; Dean, K.; Cook, W. Water absorption by uncrosslinked polymers, networks and IPNs having medium to high polarity. *Polymer* **2002**, *43*, 4619−4625.

(29) Pandiyan, S.; Krajniak, J.; Samaey, G.; Roose, D.; Nies, E. A molecular dynamics study of water transport inside an epoxy polymer matrix. *Comput. Mater. Sci.* **2015**, *106*, 29−37.

(30) Vrentas, J. S.; Vrentas, C. M. J. *Diffusion and Mass Transfer*; CRC Press, Taylor & Francis Group: Boca Raton, 2013.

(31) Toscano, A.; Pitarresi, G.; Scafidi, M.; Di Filippo, M.; Spadaro, G.; Alessi, S. Water diffusion and swelling stresses in highly crosslinked epoxy matrices. *Polym. Degrad. Stab.* **2016**, *133*, 255−263.

(32) Garden, L.; Pethrick, R. A., A dielectric study of water uptake in epoxy resin systems. *J. Appl. Polym. Sci.* **2017**, *134* (). DOI: 10.1002/app.44717

(33) Zou, C.; Fu, M.; Fothergill, J. C.; Rowe, S. W. In *Influence of Absorbed Water on the Dielectric Properties and Glass-Transition Temperature of Silica-Filled Epoxy Nanocomposites*, IEEE Conference on Electrical Insulation and Dielectric Phenomena, 15−18 Oct, 2006; pp 321−324.

(34) Alhabill, F. N.; Andritsch, T.; Vaughan, A. S. In *On Water Absorption and Its Impact on the Dielectric Spectra of Epoxy Network with Different Stoichiometries*, IEEE Conference on Electrical Insulation and Dielectric Phenomenon (CEIDP), 22−25 Oct, 2017; pp 469−475.

(35) Miszczyk, A.; Darowicki, K. Water uptake in protective organic coatings and its reflection in measured coating impedance. *Prog. Org. Coat.* **2018**, *124*, 296−302.

DOI: 10.1021/acsomega.9b00859
ACS Omega 2019, 4, 10799−10808

(36) Crank, J. *The Mathematics of Diffusion / by J. Crank*; Clarendon Press: Oxford [England], 1975.
(37) Rogers, C. Solubility and Diffusivity. *Phys. Chem. Org. Solid State* **1965**, *2*, 509−635.
(38) Moiseev, Y. V.; Markin, V. S.; Gennadii, E. Z. Chemical Degradation of Polymers in Corrosive Liquid Media. *Russ. Chem. Rev.* **1976**, *45*, 246.
(39) Sefton, M. V.; Merrill, E. W. Effect of stress transfer modified swelling on diffusion in polymers. *Nature* **1975**, *255*, 394.
(40) Bornmann, J. A.; Wolf, C. J. Reaction of nitric acid with a solid epoxy resin. *J. Polym. Sci., Polym. Chem. Ed.* **1984**, *22*, 851−856.
(41) Kotnarowska, D. Influence of ultraviolet radiation and aggressive media on epoxy coating degradation. *Prog. Org. Coat.* **1999**, *37*, 149−159.
(42) Xiao, G. Z.; Shanahan, M. E. R. Water absorption and desorption in an epoxy resin with degradation. *J. Polym. Sci., Part B: Polym. Phys.* **1997**, *35*, 2659−2670.
(43) Netravali, A. N.; Fornes, R. E.; Gilbert, R. D.; Memory, J. D. Thermogravimetric analysis of water-epoxy interaction. *J. Appl. Polym. Sci.* **1986**, *31*, 1531−1535.
(44) Reed, T. F.; Bair, H. E.; Vadimsky, R. G. The Causes of Pitting and Haze on Molded ABS Plastic Surfaces. In *Recent Advances in Polymer Blends, Grafts, and Blocks*; Sperling, L. H., Ed.; Springer: Boston, MA, 1974; pp 359−373.
(45) Technologies, K. *Keysight 16451B Dielectric Test Fixture Operation and Service Manual*; Keysight Technologies, 2014.
(46) Lemay, J. D.; Swetlin, B. J.; Kelley, F. N. Structure and Fracture of Highly Cross-linked Networks. In *Characterization of Highly Cross-linked Polymers*; American Chemical Society, 1984; Vol. *243*, pp 165−183.

DOI: 10.1021/acsomega.9b00859
ACS Omega 2019, 4, 10799−10808